

Observability Analysis of Graph SLAM-Based Joint Calibration of Multiple Microphone Arrays and Sound Source Localization

Yuanzheng He, Jiang Wang, Daobilige Su, Kazuhiro Nakadai, Junfeng Wu, Shoudong Huang, Youfu Li, and He Kong

Abstract—Multiple microphone arrays have many applications in robot audition, including sound source localization, audio scene perception and analysis, etc. However, accurate calibration of multiple microphone arrays remains a challenge because there are many unknown parameters to be identified, including the Euler angles, geometry, asynchronous factors between the microphone arrays. This paper is concerned with joint calibration of multiple microphone arrays and sound source localization using graph simultaneous localization and mapping (SLAM). By using a Fisher information matrix (FIM) approach, we focus on the observability analysis of the graph SLAM framework for the above-mentioned calibration problem. We thoroughly investigate the identifiability of the unknown parameters, including the Euler angles, geometry, asynchronous effects between the microphone arrays, and the sound source locations. We establish necessary/sufficient conditions under which the FIM and the Jacobian matrix have full column rank, which implies the identifiability of the unknown parameters. These conditions are closely related to the variation in the motion of the sound source and the configuration of microphone arrays, and have intuitive and physical interpretations. We also discover several scenarios where the unknown parameters are not uniquely identifiable. All theoretical findings are demonstrated using simulation data.

I. INTRODUCTION

Microphone array-based robot audition systems can be used for a range of applications, such as sound source localization, active multi-mode perception, speech separation, and recognition of multiple sound sources [1]-[8]. However, accurate calibration of microphone array-based robotic auditory sensors, as for other sensing modalities such as camera and LIDAR [9]-[12], is crucial for satisfactory performance. Hence, calibration of microphone array-based robot audition systems have received much attention in the recent literature.

This paper is accepted to and going to be presented at 2023 IEEE/SICE International Symposium on System Integrations, Atlanta, USA. Corresponding author: H. Kong. Y. He and J. Wang contributed equally to this work. Y. He, J. Wang, and H. Kong are with the Shenzhen Key Laboratory of Biomimetic Robotics and Intelligent Systems, Department of Mechanical and Energy Engineering, Southern University of Science and Technology (SUSTech), Shenzhen, 518055, China; they are also affiliated with the Guangdong Provincial Key Laboratory of Human-Augmentation and Rehabilitation Robotics in Universities, SUSTech, Shenzhen, 518055, China (e-mail: 12132259@mail.sustech.edu.cn; 12132297@mail.sustech.edu.cn; kongh@sustech.edu.cn). D. Su is with College of Engineering, China Agricultural University, Beijing, China (email: sudao@cau.edu.cn). K. Nakadai is with the Department of Systems and Control Engineering, Tokyo Institute of Technology, Tokyo, Japan (email: nakadai@ra.sc.e.titech.ac.jp). J. Wu is with the School of Data Science, The Chinese University of Hong Kong, Shenzhen, Shenzhen, P. R. China (email: junfengwu@cuhk.edu.cn). S. Huang is with the Robotics Institute, University of Technology Sydney, Sydney, Australia (email: shoudong.huang@uts.edu.au). Y. Li is with the Department of Mechanical Engineering, City University of Hong Kong, Hong Kong SAR, China (email: meyfli@cityu.edu.hk).

For example, a calibration technique was proposed in [13], which allowed estimating microphone position, source position and time offset independent of the calibration signal. Some researchers have tried to use frameworks combining SLAM and beamforming algorithms to perform online calibration of asynchronous microphones without many measurements of transfer functions [14]-[15]. For microphone arrays with asynchronous effects (i.e., clock difference and initial time offset), a systematic examination and observability analysis of SLAM-based microphone array calibration and sound source localization was presented in [16]-[18] via a FIM approach. However, the above-mentioned methods are only applicable for calibrating a single microphone array.

Methods for estimating the parameters of multiple microphone arrays have been presented in [19]-[22]. Nevertheless, these methods assumed that the hardware synchronization or orientations of the microphone arrays were known, and only considered scenarios in 2-dimensions (2D). For calibrating multiple microphone arrays, it is necessary to consider not only the geometry and asynchronous effects among the arrays, but also the orientations of microphone arrays.

Simultaneous calibration of positions, orientations, time offsets among multiple microphone arrays and sound source location was explored in [23]. In the former work, a combined cost function has been proposed that can allow for estimating the array position, orientation, and time offset concurrently, by using direction of arrival (DOA) information and the time difference of arrival (TDOA) measurements among microphone arrays. However, a thorough analysis regarding the parameter observability in the joint calibration of multiple microphone arrays and sound source localization is still lacking.

In this study, we will use graph SLAM as a general framework for the above identification question, and concentrate on the parameter identifiability of the corresponding SLAM problem. By using a FIM approach, we thoroughly investigate the identifiability of the unknown parameters, including the Euler angles, geometry, asynchronous effects between the microphone arrays, and the sound source locations. We establish necessary/sufficient conditions under which the FIM and the Jacobian matrix have full column rank, which implies the identifiability of the unknown parameters. These conditions are closely related to the variation in the motion of the sound source and the configuration of microphone arrays, and have intuitive and physical interpretations. We also discover several scenarios where the unknown parameters are not uniquely identifiable. All theoretical findings have

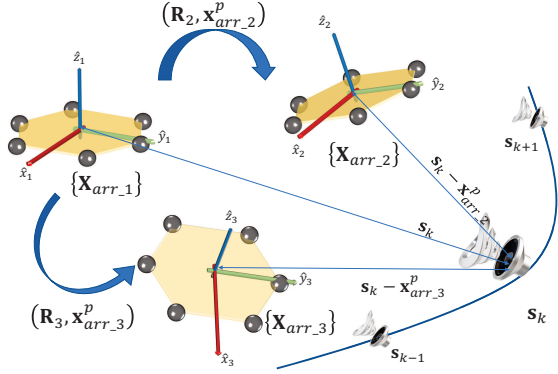


Fig. 1. Geometry of the problem setup and graph-based SLAM framework

been validated using simulation data. For readability, most proofs of the theoretical results are put in the Appendix.

Notation: Denote x , \mathbf{x} , and \mathbf{X} as scalars, vectors, and matrices, respectively. \mathbf{X}^T represents the transpose of matrix \mathbf{X} . \mathbf{I}_n stands for the identity matrix of n dimensions. \mathbb{R}^n denotes the n -dimensional Euclidean space. $[a_1; \dots; a_n]$ denotes $[a_1^T; \dots; a_n^T]^T$, where a_1, \dots, a_n are scalars/vectors/matrices with proper dimensions. $\text{diag}_n(\mathbf{A})$ denotes a block diagonal matrix with \mathbf{A} as block diagonal entries for n times; $\text{diag}(\mathbf{A}, \mathbf{B})$ denotes a block diagonal matrix with \mathbf{A} and \mathbf{B} as its block diagonal entries; and $\mathbf{0}_{a \times b}$ as a matrix of dimension $a \times b$ with its all entries as 0. $\mathbf{X} > 0$ means that \mathbf{X} is a positive definite matrix. We denote $\|\mathbf{x}\|_{\mathbf{P}}^2 = \mathbf{x}^T \mathbf{P} \mathbf{x}$. Vectors/matrices, with dimensions not explicitly stated, are assumed to be algebraically compatible.

II. PRELIMINARIES AND PROBLEM STATEMENT

A. Graph SLAM for Multiple Microphone Arrays Calibration

In a calibration scene containing N distributed microphone arrays, the microphone arrays capture K consecutive acoustic signals emitted by a single acoustic source at several spatial positions. As shown in Fig. 1 (here we take $N=3$ as an example), in this paper, simultaneous sound source localization and multiple microphone arrays calibration are performed in a graph-based SLAM framework with three microphone arrays and one moving source.

In Fig. 1, \mathbf{x}_{arr-j}^p represents the location of the i -th microphone array in the global reference frame, and any two of arrays are in different positions. We assume that there is a local reference frame $\{\mathbf{x}_{arr-j}\}$ attached to every microphone array; we choose $\{\mathbf{x}_{arr-1}\}$ as the global reference frame; \mathbf{R}_i is the rotation matrix of reference frame $\{\mathbf{x}_{arr-1}\}$ to the frame $\{\mathbf{x}_{arr-j}\}$ with the rotation angle vector $\mathbf{x}_{arr-j}^\theta$; \mathbf{s}^k is the sound source position at time t^k , $k = 1, \dots, K$, with respect to (w.r.t.) $\{\mathbf{x}_{arr-1}\}$, where K is the total number of time steps; d_i^k is the distance between the i -th microphone array and the sound source at time instance t^k . Note that in the calibration process, the multiple microphone arrays remain static while the sound source moves around in the environment.

Here we consider the most general scenario where there are starting time offset and clock drift among different microphone arrays (we assume that the configuration of each microphone array, including its geometry, is known). When the sound source sends the k -th acoustic signal, the DOA information, i.e., the direction vector of sound source relative to the i -th microphone array frame $\{\mathbf{x}_{arr-j}\}$ is obtained as follows:

$$\mathbf{d}_{i1}^k = \mathbf{R}_i^T \frac{\mathbf{s}^k - \mathbf{x}_{arr-j}^p}{d_i^k}. \quad (1)$$

Denote d_i^k , for $i = 1, \dots, N$, as the distance between the i -th microphone array and the sound source at the k -th sampling instant. The TDOA information between the i -th and the first microphone arrays can be expressed as follows:

$$T_{i1}^k = \frac{d_i^k}{c} - \frac{d_1^k}{c} + x_{arr-j}^\tau + k \Delta_t x_{arr-j}^\delta \quad (2)$$

for $i = 2, \dots, N$, where c represents the sound speed in the air; the scalar (unknown) constant variables x_{arr-j}^τ and x_{arr-j}^δ represent the starting time offset and the clock difference per second of each microphone array, respectively; Δ_t is the time interval between two consecutive sound signals. As mentioned above, the first microphone array is used as the reference, hence

$$\mathbf{x}_{arr-1}^p = \mathbf{0}, \mathbf{x}_{arr-1}^\theta = \mathbf{0}, x_{arr-1}^\tau = 0, x_{arr-1}^\delta = 0.$$

The Euler angles, starting time offsets, and clock differences of the microphone arrays will be determined along with the source positions in the calibration process.

The location and the rotation angle vector of i -th microphone array (where $i = 2, \dots, N$), i.e., \mathbf{x}_{arr-j}^p and $\mathbf{x}_{arr-j}^\theta$, can be expressed as:

$$\mathbf{x}_{arr-j}^p = [x_{arr-j}^x; x_{arr-j}^y; x_{arr-j}^z], \mathbf{x}_{arr-j}^\theta = [\theta_{arr-j}^x; \theta_{arr-j}^y; \theta_{arr-j}^z],$$

respectively, where θ_{arr-j}^x , θ_{arr-j}^y , and θ_{arr-j}^z take values in the range of $[0, 2\pi]$, $[0, \pi]$, and $[0, 2\pi]$, respectively. Denote the unknown parameters w.r.t. the i -th microphone array as:

$$\mathbf{x}_{arr-j} = [\mathbf{x}_{arr-j}^p; \mathbf{x}_{arr-j}^\theta; x_{arr-j}^\tau; x_{arr-j}^\delta].$$

Hence, all the unknown parameters w.r.t. the microphone arrays are:

$$\mathbf{x}_{arr} = [\mathbf{x}_{arr-2}; \dots; \mathbf{x}_{arr-N}].$$

Denote the sound source position at time t^k , $k = 1, \dots, K$ as:

$$\mathbf{s}^k = [s_x^k; s_y^k; s_z^k].$$

Thus, all unknown parameters to be identified are:

$$\mathbf{x} = [\mathbf{x}_{arr}; \mathbf{s}^1; \dots; \mathbf{s}^K].$$

We denote the ideal TDOA and DOA measurement information at the k -th time instance as:

$$\mathbf{z}^k = [T_{21}^k; \mathbf{d}_{21}^k; T_{31}^k; \mathbf{d}_{31}^k; \dots; T_{N1}^k; \mathbf{d}_{N1}^k] \in \mathbb{R}^{4(N-1)}. \quad (3)$$

The real values of DOA and TDOA measurements at time k are also subject to the influence of Gaussian noise as follows:

$$\mathbf{y}^k = \mathbf{z}^k + \mathbf{v}^k \quad (4)$$

where \mathbf{z}^k is defined in (3), $\mathbf{v}^k \sim \mathcal{N}(0, \mathbf{P})$, with $\mathbf{P} > 0 \in \mathbb{R}^{4(N-1) \times 4(N-1)}$. We assume that the sound source relative position between two consecutive time steps can be measured with Gaussian noise, i.e.,

$$\mathbf{s}_\Delta^k = \mathbf{s}^{k+1} - \mathbf{s}^k + \mathbf{w}^k \quad (5)$$

where $k = 1, \dots, K-1$, $\mathbf{w}^k \sim \mathcal{N}(0, \mathbf{Q})$, with $\mathbf{Q} > 0 \in \mathbb{R}^{3 \times 3}$. We combine the relative position measurements, the TDOA, and DOA measurements as:

$$\mathbf{m} = [\mathbf{y}_1; \mathbf{s}_1^\Delta; \mathbf{y}_2; \mathbf{s}_2^\Delta; \dots; \mathbf{y}_{K-1}; \mathbf{s}_{K-1}^\Delta; \mathbf{y}_K]$$

where \mathbf{s}_k^Δ and \mathbf{y}_k are defined in (5) and (4), respectively. Then the models in (4)-(5) can be rewritten in a compact form as:

$$\mathbf{m} = \mathbf{g}(\mathbf{x}) + \gamma \quad (6)$$

where $\mathbf{g}(\mathbf{x})$ is the combined observation model, and $\gamma \sim \mathcal{N}(0, \mathbf{W})$ is the noise of combined observations with

$$\mathbf{W} = \text{diag}(\text{diag}_{K-1}(\mathbf{P}, \mathbf{Q}), \mathbf{P}). \quad (7)$$

Based on the above discussions, our focus is to identify the parameters of multiple microphone arrays (microphone arrays positions, orientations, time offsets, and clock offsets) and sound source positions. As shown in Fig. 1, the graph-based SLAM framework is a feasible solution to the above problems by treating the moving sound source as a robot and the multiple microphone arrays as landmarks [24]. As in [16]-[17], the parameter identification problem for asynchronous multiple microphone arrays can be treated as the following standard least squares (LS) problem using graph SLAM:

$$\arg \min_{\hat{\mathbf{x}}} \|\mathbf{m} - \mathbf{g}(\hat{\mathbf{x}})\|_{\mathbf{W}^{-1}}^2 \quad (8)$$

where $\hat{\mathbf{x}}$ represents the estimate of all the unknown parameters. The measurements obtained by different microphone arrays constitute the spatial constraints and can be included in the above LS to improve estimation accuracy (due to limited space, we will not elaborate on these details in the remainder of the paper).

B. The Corresponding FIM and Problem Statement

By using the FIM approach, we know that the observability of the graph-based SLAM problem described earlier depends on whether the FIM is non-singular [18]. For non-random vector parameter estimation, the FIM of an unbiased estimator is defined as

$$\mathbf{I}_{FIM} \triangleq E\{[\nabla_{\mathbf{x}} \ln \Lambda(\mathbf{x})][\nabla_{\mathbf{x}} \ln \Lambda(\mathbf{x})]^T\} \quad (9)$$

where $\Lambda(\mathbf{x}) \triangleq p(\mathbf{m}|\mathbf{x})$ is the likelihood function, and the partial derivatives should be calculated at the true value of \mathbf{x} [25, chap. 2]. By following similar arguments as those in [26] and [27], the FIM in (9) for models in (6)-(7) can be formulated as

$$\mathbf{I}_{FIM} = \mathbf{J}^T \mathbf{W}^{-1} \mathbf{J} \quad (10)$$

where \mathbf{J} is the Jacobian matrix of the function $\mathbf{g}(\bullet)$ in (6) w.r.t. \mathbf{x} [28, pp. 569], and its explicit expression will be given later in the paper (see in (11)). When $\mathbf{W} > 0$, one has that

$$\text{rank}(\mathbf{J}) = \text{rank}(\mathbf{I}_{FIM}).$$

The question of interests is formally stated as follows.

Problem: Given the problem setup described as above, find conditions under which the FIM \mathbf{I}_{FIM} defined in (9) is non-singular, or equivalently, the Jacobian matrix \mathbf{J} is of full column rank.

III. MAIN RESULTS

By leveraging the structure of the Jacobian matrix \mathbf{J} associated with the SLAM formulation, we next establish necessary/sufficient conditions for the non-singularity of the \mathbf{I}_{FIM} and the observability of the SLAM problem. In addition, we will reveal some special cases when the Jacobian matrix or FIM cannot have full column rank.

A. Main Results

From the definition of the Jacobian matrix [28, pp. 569], we know that $\mathbf{J} \in \mathbb{R}^{g_1 \times g_2}$, $g_1 = 4(N-1)K + 3(K-1)$, $g_2 = 8(N-1) + 3K$. From (9)-(10), a necessary and sufficient condition for \mathbf{I}_{FIM} to be nonsingular is that \mathbf{J} has full column rank. For \mathbf{J} to be of full column rank, it is necessary that

$$4(N-1)K + 3(K-1) \geq 8(N-1) + 3K \\ \implies K \geq \left\lceil 2 + \frac{3}{4(N-1)} \right\rceil,$$

where $\lceil \cdot \rceil$ stands for the ceiling operation generating the least integer not less than the number within the operator. We then have the following results.

Proposition: The Jacobian \mathbf{J} can be written as

$$\mathbf{J} = \begin{bmatrix} \mathbf{L}^1 & \mathbf{T}^1 & \mathbf{0}_{4\tilde{N} \times 3} & \dots & \mathbf{0} & \mathbf{0} \\ \mathbf{0}_{3 \times 8\tilde{N}} & -\mathbf{I}_3 & \mathbf{I}_3 & \dots & \mathbf{0} & \mathbf{0} \\ \mathbf{L}^2 & \mathbf{0}_{4\tilde{N} \times 3} & \mathbf{T}^2 & \dots & \mathbf{0} & \mathbf{0} \\ \mathbf{0} & \mathbf{0} & -\mathbf{I}_3 & \dots & \mathbf{0} & \mathbf{0} \\ \vdots & \vdots & \vdots & \ddots & \vdots & \vdots \\ \mathbf{L}^{K-1} & \mathbf{0} & \mathbf{0} & \dots & \mathbf{T}^{K-1} & \mathbf{0} \\ \mathbf{0} & \mathbf{0} & \mathbf{0} & \dots & -\mathbf{I}_3 & \mathbf{I}_3 \\ \mathbf{L}^K & \mathbf{0} & \mathbf{0} & \dots & \mathbf{0} & \mathbf{T}^K \end{bmatrix} \quad (11)$$

$\underbrace{\hspace{15em}}_{\mathbf{J}_1} \quad \underbrace{\hspace{15em}}_{\mathbf{J}_2 = [\mathbf{J}_2^1 \quad \mathbf{J}_2^2 \dots \mathbf{J}_2^{K-1} \quad \mathbf{J}_2^K]}$

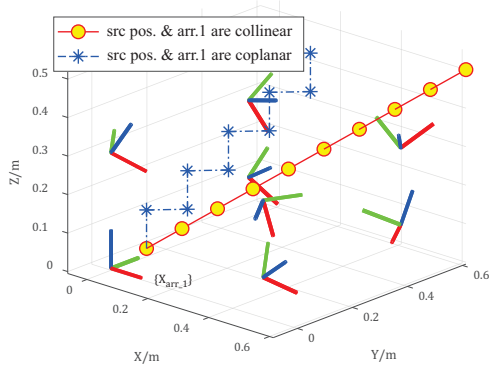
where $\tilde{N} = N-1$, expressions of \mathbf{L}^k , \mathbf{T}^k , for $k = 1, \dots, K$, can be found in (15) and (19).

Theorem 1: The Jacobian matrix \mathbf{J} is of full column rank if and only if the following matrix

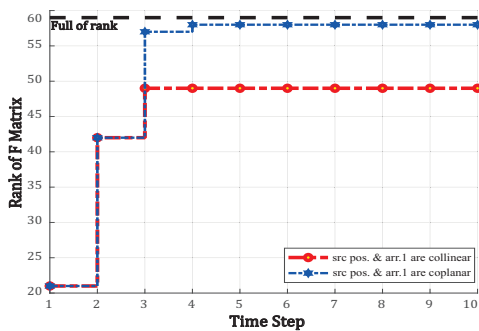
$$\mathbf{F} = \begin{bmatrix} \mathbf{L}^1 & \mathbf{T}^1 \\ \mathbf{L}^2 & \mathbf{T}^2 \\ \vdots & \vdots \\ \mathbf{L}^K & \mathbf{T}^K \end{bmatrix}$$

$\underbrace{\hspace{10em}}_{\mathbf{L}} \quad \underbrace{\hspace{10em}}_{\mathbf{T}}$

is of full column rank.



(a)



(b)

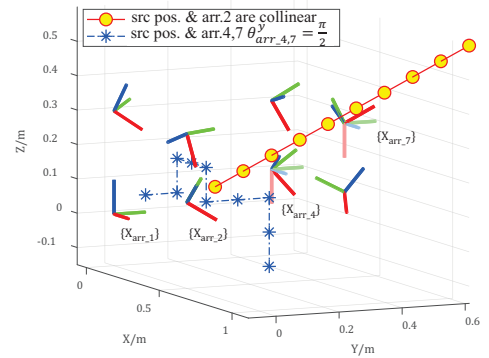
Fig. 3. The sound source remains co-linear or co-planar with $\{\mathbf{x}_{arr-1}\}$ during the movement. (a) Geometric relationship between the source and the microphone arrays during the movement. (b) Variation of the \mathbf{F} matrix rank with the movement of the source.

shown in Fig. 2(a). The variation of \mathbf{F} matrix rank with time steps is shown in Fig. 2(b). It can be seen that as time steps increase and the sound source moves along the two trajectories, the \mathbf{F} matrix gradually becomes full column rank which indicates that the Jacobian matrix also gradually becomes full column rank. Based on Theorem 3, since $rank(\mathbf{M}_{2,T}) = 11$ and $rank(diag(\bar{\mathbf{L}}_i)) = 48$, $i = 3, 4, \dots, 8$, the Jacobian matrix is of full column rank. At the moment when the Jacobian matrix becomes full column rank, it can be verified that $rank(diag(\bar{\mathbf{L}}_i)) = 56$, $i = 2, 3, \dots, 8$, and $rank(\bar{\mathbf{T}}) = 3$. Hence, the simulations presented so far based on the theorems worked properly as expected. It is worth noting that the sound source positions are not always in the same plane or same line. Therefore, the Jacobian matrix is of full column rank in general.

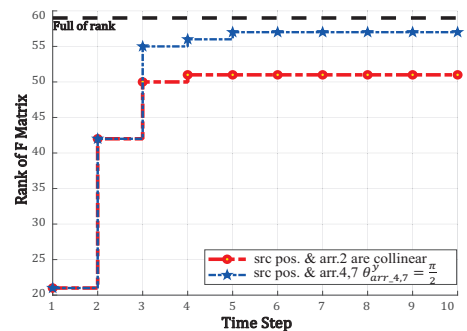
B. Unobservable Cases

Several unobservable scenarios are presented in the following to verify the conclusions in Theorems 4-5.

(i) For the Jacobian matrix to have full column rank, it is necessary that the time steps are greater than or equal to 3 so that the number of rows of the Jacobian matrix is greater than the number of columns. As can be seen from Fig. 2(b), when the number of time steps is greater than or equal to 3 but less than 5, the Jacobian matrix is not of full column rank. This reflects that the system is unobservable when the number of time steps is less than 5.



(a)



(b)

Fig. 4. The sound source remains co-linear with $\{\mathbf{x}_{arr-2}\}$ or $\theta_{arr-4,7}^y = \pi/2$ during the movement. (a) Geometric relationship between the source and the microphone arrays during the movement. (b) Variation of the \mathbf{F} matrix rank with the movement of the source.

(ii) For the trajectories of the sound source shown in Fig. 3(a), the first case is that the sound source stays co-linear with $\{\mathbf{x}_{arr-1}\}$ during the moving process, and the second case is that the sound source remains co-planar with $\{\mathbf{x}_{arr-1}\}$. From Fig. 3(b), it can be seen that both are permanently unobservable due to the lack of information.

(iii) For the sound source trajectories shown in Fig. 4(a), the first case is that the sound source keeps co-linear with the origin of $\{\mathbf{x}_{arr-2}\}$ during the movement. In the second case, the Euler angles θ_{arr-4}^y and θ_{arr-7}^y of $\{\mathbf{x}_{arr-4}\}$ and $\{\mathbf{x}_{arr-7}\}$ are $\frac{\pi}{2}$, and the sound source travels along the route of the observable scenario mentioned in case 1 of Fig. 2(a). The rotation angle is at the singular point of observation, rendering the system unobservable. Hence, the simulations presented above validate the conclusions in Theorems 4-5.

V. CONCLUSION

This paper is concerned with the observability analysis of graph SLAM-based joint calibration of multiple microphone arrays and sound source localization. Via a FIM approach, we thoroughly investigate the identifiability of the unknown parameters, including the Euler angles, geometry, asynchronous effects between the microphone arrays, and the sound source locations. We establish necessary/sufficient conditions under which the FIM and the Jacobian matrix have full column rank, which implies the identifiability of the unknown parameters. These conditions are closely related

to the variation in the motion of the sound source and the configuration of microphone arrays, and have intuitive and physical interpretations. Based on these conditions, we also find some special cases when the Jacobian matrix does not have full column rank, and provide some geometric and physical interpretations. Extensive simulations have been conducted to demonstrate the theoretical findings. The focus of our current and further work is to develop and validate calibration algorithms for multiple microphone arrays.

VI. ACKNOWLEDGMENT

This work was supported by the Science, Technology, and Innovation Commission of Shenzhen Municipality [Grant No. ZDSYS20200811143601004].

REFERENCES

- [1] F. Grondin and F. Michaud, Lightweight and optimized sound source localization and tracking methods for open and closed microphone array configurations, *Robotics and Autonomous Systems*, Vol. 113, pp. 63–80, 2019.
- [2] L. Wang, R. Sanchez-Matilla, and A. Cavallaro, Tracking a moving sound source from a multi-rotor drone, *Proc. of the IEEE/RSJ IROS*, pp. 2511–2516, 2018.
- [3] C. Evers and P. A. Naylor, Acoustic SLAM, *IEEE/ACM Trans. on Audio, Speech, and Language Processing*, Vol. 26, No. 9, pp. 1484–1489, 2018.
- [4] M. Strauss, P. Mordel, V. Miguet, and A. Deleforge, DREGON: Dataset and methods for UAV-embedded sound source localization, *Proc. of the IEEE/RSJ IROS*, pp. 5735–5742, 2018.
- [5] Z. Shi, X. Chang, C. Yang, Z. Wu, and J. Wu, An acoustic-based surveillance system for amateur drones detection and localization, *IEEE Trans. on Vehicular Technology*, Vol. 69, No. 3, pp. 2731–2739, 2020.
- [6] S. Eiffert, N. Wallace, H. Kong, N. Pirmarzdashti, and S. Sukkariéh, Resource and response aware path planning for long term autonomy of ground robots in agriculture, *Field Robotics*, Vol. 2, pp. 1–33, 2022.
- [7] J. Wakulicz, H. Kong, and S. Sukkariéh, Active information acquisition under arbitrary unknown disturbances, *Proc. of the IEEE ICRA*, Vol. 96, pp. 8429–8435, 2021.
- [8] C. Rascon and I. Meza, Localization of sound sources in robotics: A review, *Robotics and Autonomous Systems*, Vol. 96, pp. 184–210, 2017.
- [9] J. Lv, X. Zuo, K. Hu, J. Xu, G. Huang, and Y. Liu, Observability-aware intrinsic and extrinsic calibration of LiDAR-IMU systems, *IEEE Trans. on Robotics*, Early access, pp. 1–20, 2022.
- [10] J. Brown, D. Su, H. Kong, S. Sukkariéh, and E. Kerrigan, Improved noise covariance estimation in visual servoing using an autocovariance least-squares approach, *Mechatronics*, Vol. 68, pp. 1–10, 2020.
- [11] M. Liu, Y. Li, and H. Liu, Robust 3-D gaze estimation via data optimization and saliency aggregation for mobile eye-tracking systems, *IEEE Trans. on Instrumentation and Measurement*, Vol. 70, Article ID. 5008010, pp. 1–10, 2021.
- [12] J. Jiao, Y. Yu, Q. Liao, H. Ye, R. Fan, and M. Liu, Automatic calibration of multiple 3D lidars in urban environments, *Proc. of the IEEE/RSJ IROS*, pp. 15–20, 2019.
- [13] F. Perrodin, J. Nikolic, J. Busset, and R. Siegwart, Design and calibration of large microphone arrays for robotic applications, *Proc. of the IEEE/RSJ IROS*, pp. 4596–4601, 2012.
- [14] H. Miura, T. Yoshida, K. Nakamura, and K. Nakadai, SLAM-based online calibration of asynchronous microphone array for robot audition, *Proc. of the IEEE/RSJ IROS*, pp. 524–529, 2011.
- [15] H. Miura, T. Yoshida, K. Nakamura, and K. Nakadai, SLAM-based online calibration for asynchronous microphone array, *Advanced Robotics*, Vol. 26, No. 17, pp. 1941–1965, 2012.
- [16] D. Su, T. Vidal-Calleja, and J. V. Miro, Simultaneous asynchronous microphone array calibration and sound source localisation, *Proc. of the IEEE/RSJ IROS*, pp. 5561–5567, 2015.
- [17] D. Su, T. Vidal-Calleja, and J. V. Miro, Asynchronous microphone arrays calibration and sound source tracking, *Autonomous Robots*, Vol. 44, No. 2, pp. 183–204, 2020.
- [18] D. Su, H. Kong, S. Sukkariéh, and S. Huang, Necessary and sufficient conditions for observability of SLAM-based TDOA sensor array calibration and source localization, *IEEE Trans. on Robotics*, Vol. 37, No. 5, pp. 1451–1468, 2021.
- [19] A. Plinge and G. A. Fink, Geometry calibration of multiple microphone arrays in highly reverberant environments, *Proc. of the Int. Workshop on Acoustic Signal Enhancement*, pp. 243–247, 2014.
- [20] A. Plinge, F. Jacob, R. Haeb-Umbach, and G. A. Fink, Acoustic microphone geometry calibration: An overview and experimental evaluation of state-of-the-art algorithms, *IEEE Signal Processing Magazine*, Vol. 33, No. 4, pp. 14–29, 2016.
- [21] A. Plinge, G. A. Fink, and S. Gannot, Passive online geometry calibration of acoustic sensor networks, *IEEE Signal Processing Letters*, Vol. 24, No. 3, pp. 324–328, 2017.
- [22] S. Woźniak and K. Kowalczyk, Passive joint localization and synchronization of distributed microphone arrays, *IEEE Signal Processing Letters*, Vol. 26, No. 2, pp. 292–296, 2019.
- [23] C. Sugiyama, K. Itoyama, K. Nishida, and K. Nakadai, Simultaneous calibration of positions, orientations, and time offsets, among multiple microphone arrays, *Proc. of the IEEE Int. Conference on Autonomous Systems*, pp. 1–5, 2021.
- [24] G. Grisetti, R. Kümmerle, C. Stachniss, and W. Burgard, A tutorial on graph-based SLAM, *IEEE Intelligent Transportation Systems Magazine*, Vol. 2, No. 4, pp. 31–43, 2010.
- [25] Y. Bar-Shalom, X. R. Li, and T. Kirubarajan, Estimation with applications to tracking and navigation: Theory algorithms and software. New York: Wiley, 2004.
- [26] Z. Wang and G. Dissanayake, Observability analysis of SLAM using Fisher information matrix, *Proc. of the Int. Conf. on Control, Automation, Robotics, and Vision*, pp. 1242–1247, 2008.
- [27] S. Huang and G. Dissanayake, A critique of current developments in simultaneous localization and mapping, *Int. Journal of Advanced Robotic Systems*, Vol. 13, No. 5, pp. 1–13, 2016.
- [28] B. Siciliano, L. Sciavicco, L. Villani, and G. Oriolo, Robotics: Modeling, planning, and control, Berlin, Germany: Springer, 2009.

APPENDIX

Proof of Proposition. Firstly, we note that the relative position of the sound source satisfies

$$\mathbf{s}_{\Delta}^{k-1} = \mathbf{s}^k - \mathbf{s}^{k-1} + \mathbf{w}^{k-1}$$

whose corresponding Jacobian matrices are

$$\frac{\partial \mathbf{s}_{\Delta}^{k-1}}{\partial \mathbf{s}^{k-1}} = -\mathbf{I}_3, \quad \frac{\partial \mathbf{s}_{\Delta}^{k-1}}{\partial \mathbf{s}^k} = \mathbf{I}_3.$$

Secondly, for $i = 2, \dots, N$, the distance between the i -th microphone array and the sound source at time instance t^k can be computed as

$$d_i^k = \sqrt{(\Delta x_i^k)^2 + (\Delta y_i^k)^2 + (\Delta z_i^k)^2}$$

where $\Delta x_i^k = s_x^k - x_{arr,i}^x$, $\Delta y_i^k = s_y^k - x_{arr,i}^y$, $\Delta z_i^k = s_z^k - x_{arr,i}^z$. When $i = 1$, i.e., for the first microphone array, we have

$$d_1^k = \sqrt{(s_x^k)^2 + (s_y^k)^2 + (s_z^k)^2}. \quad (14)$$

Denote $\mathbf{L}^k = \frac{\partial \mathbf{z}^k}{\partial \mathbf{x}_{arr}}$, i.e., \mathbf{L}^k is the derivative of \mathbf{z}^k (the measurements at the time step t^k) w.r.t. \mathbf{x}_{arr} . Based on the DOA and TDOA information in (1)–(2), we then have:

$$\mathbf{L}^k = \frac{\partial \mathbf{z}^k}{\partial \mathbf{x}_{arr}} = [\mathbf{J}_{arr,2}^k, \dots, \mathbf{J}_{arr,N}^k] \in \mathbb{R}^{4\tilde{N} \times 8\tilde{N}} \quad (15)$$

where for $i = 2, \dots, N$, and $k = 1, \dots, K$, and only entries of $\mathbf{J}_{arr,i}^k$ on its $(4i - 7 : 4i - 4)$ rows are nonzero. Denote $\mathbf{H}_i^k, \mathbf{U}_i^k$ as the partial derivative of TDOA and DOA w.r.t. microphone array position, respectively; denote \mathbf{V}_i^k as the

where

$$\begin{cases} \mathbf{k} = [1; 2; \dots; K], \mathbf{M}_{h,j} = [\mathbf{h}_i^1; \mathbf{h}_i^2; \dots; \mathbf{h}_i^K], \\ \mathbf{M}_{U,j} = [\mathbf{U}_i^1; \mathbf{U}_i^2; \dots; \mathbf{U}_i^K], \mathbf{M}_{V,j} = [\mathbf{V}_i^1; \mathbf{V}_i^2; \dots; \mathbf{V}_i^K], \\ \mathbf{t}_K = \left[\begin{array}{c} \left(\frac{s^1}{cd_1^k}\right)^\top; \left(\frac{s^2}{cd_1^k}\right)^\top; \left(\frac{s^K}{cd_1^k}\right)^\top \end{array} \right]. \end{cases}$$

We further perform the following elementary operations on $\bar{\mathbf{F}}_{arr,j}$, $i = 2, 3, \dots, N$:

- (i) dividing the fourth column block by Δ_i ;
- (ii) for $k = 2, 3, \dots, K$, deducing the k -th row by the first row;
- (iii) transforming the elements in the first row (except the third one) to zero by the third column block (the first element therein equals 1 while the other elements equal zero after the elementary operations listed above);
- (iv) for $k = 3, 4, \dots, K$, deducing the k -th row by the second row multiplied by $(k-1)$;
- (v) transforming the elements in the second row (except the fourth one) to zero by the fourth column block (the second element therein equals 1 while the other elements equal zero after the elementary operations listed above);
- (vi) moving column blocks 3 and 4 to columns blocks 1 and 2, respectively.

After the above operations, we obtain

$$\bar{\mathbf{F}}'_{arr,j} = [\bar{\mathbf{L}}_i \quad \bar{\mathbf{T}}]$$

where $\bar{\mathbf{L}}_i$ and $\bar{\mathbf{T}}$ are shown in (13) and (12), respectively. With the above elementary transformations, we have

$$\bar{\mathbf{F}} \sim \bar{\mathbf{F}}' = \begin{bmatrix} \bar{\mathbf{L}}_2 & & & \bar{\mathbf{T}} \\ & \bar{\mathbf{L}}_3 & & \bar{\mathbf{T}} \\ & & \ddots & \vdots \\ & & & \bar{\mathbf{L}}_N & \bar{\mathbf{T}} \end{bmatrix}. \quad (20)$$

It holds that $rank(\mathbf{F}) = rank(\bar{\mathbf{F}}) = rank(\bar{\mathbf{F}}')$. From the structure of $\bar{\mathbf{F}}'$, we can see that the block columns containing $\bar{\mathbf{L}}_i$, $i = 2, \dots, N$, are independent of each other. A necessary condition for $\bar{\mathbf{F}}'$ to be of full column rank is that $\bar{\mathbf{L}}_i$ and $\bar{\mathbf{T}}$ are of full column rank, respectively, $i = 2, \dots, N$. This completes the proof. ■

Proof of Theorem 3. Here we take $j = 2$ as an example. For $\bar{\mathbf{F}}'$, we could perform elementary row block changes: for $i = 3, \dots, N$, deduce $\bar{\mathbf{L}}_i$ row block by the first-row block and obtain:

$$\begin{bmatrix} \bar{\mathbf{L}}_2 & & & \bar{\mathbf{T}} \\ -\bar{\mathbf{L}}_2 & \bar{\mathbf{L}}_3 & & \mathbf{0} \\ \vdots & & \ddots & \vdots \\ -\bar{\mathbf{L}}_2 & & & \bar{\mathbf{L}}_N & \mathbf{0} \end{bmatrix}. \quad (21)$$

Denote the submatrix of this matrix as:

$$\mathbf{M}_{2,T} = \begin{bmatrix} \bar{\mathbf{L}}_2 & \bar{\mathbf{T}} \\ \vdots & \vdots \\ -\bar{\mathbf{L}}_2 & \mathbf{0} \end{bmatrix}.$$

From the structure in (21), we can see clearly that if:

- (i) $\mathbf{M}_{2,T}$ is of full column rank, and

- (ii) $diag(\bar{\mathbf{L}}_3, \dots, \bar{\mathbf{L}}_N)$ is of full column rank,

then $\bar{\mathbf{F}}'$ will be of full column rank. Due to the fact that $rank(\mathbf{F}) = rank(\bar{\mathbf{F}}) = rank(\bar{\mathbf{F}}')$, the Jacobian matrix \mathbf{J} is of full column rank. Similarly, the same conditions hold when j equals to $3, \dots, N$. So the Jacobian matrix \mathbf{J} is of full column rank if any matrix consisting of the $(j-1)$ -th column block and the last column block in $\bar{\mathbf{F}}'$ is of full column rank, $2 \leq j \leq N$, and $\bar{\mathbf{L}}_i$ are of full column rank, $i = 2, \dots, N$ and $i \neq j$. This completes the proof. ■

Proof of Theorem 4. (i) $\bar{\mathbf{T}}$ in (12) is of full column rank only if a 3×3 matrix formed by at least one of the three-permutation of its rows is full rank. For $(\mathbf{s}^k)^\top \in R^{1 \times 3}$, $1 \leq k \leq K$, the necessary condition for $\bar{\mathbf{T}}$ to be of full column rank is $K \geq 5$. If $K < 5$, $\bar{\mathbf{T}}$ can not be of the full column rank.

(ii) Based on (14), when $\mathbf{s}^k = \lambda \mathbf{s}^{k-1}$, we could derive $\frac{\mathbf{s}^k}{d_1^k} = \frac{\mathbf{s}^{k-1}}{d_1^{k-1}}$. From the expression of $\bar{\mathbf{T}}$, we can see that $\bar{\mathbf{T}}$ cannot be of full rank if \mathbf{s}^k is proportional to each other, $k = 1, \dots, K$. In this situation, the sound source positions at all time steps are collinear (together with the origin) w.r.t. the reference microphone array frame.

(iii) If the sound source keeps moving in any planes of $x = \alpha y$, $x = \beta z$, $y = \gamma z$ w.r.t. $\{\mathbf{x}_{arr,j}\}$ at all moments, where α, β , and γ are arbitrary real numbers, the sound source position \mathbf{s}^k , $1 \leq k \leq K$, could be expressed as $[\alpha s_y^k; s_y^k; s_z^k]$, $[\beta s_z^k; s_y^k; s_z^k]$, and $[s_x^k; \gamma s_z^k; s_z^k]$, respectively. $\bar{\mathbf{T}}$ will not be of full column rank.

Specifically, if $\alpha = 0$ or $\beta = 0$ or $\gamma = 0$, the sound source position of \mathbf{s}^k will have $s_x^k = 0$, $s_y^k = 0$, and $s_z^k = 0$, respectively, i.e., YOZ, XOZ, and XOY planes. If the sound source keeps moving in the line of $x = \alpha y = \beta z$, the situation will change to (ii). This completes the proof. ■

Proof of Theorem 5. (i) If the sound source positions w.r.t. $\{\mathbf{x}_{arr,j}\}$ at all of K ($K \geq 5$) time steps are collinear, i.e., $(\mathbf{s}^k - \mathbf{x}_{arr,j}^p) = \lambda(\mathbf{s}^{k-1} - \mathbf{x}_{arr,j}^p)$ is always true. For $i \geq 2$, $k = 2, 3, \dots, K$, we can get the following expression:

$$\begin{cases} [\Delta x_i^k; \Delta y_i^k; \Delta z_i^k] = \lambda [\Delta x_i^{k-1}; \Delta y_i^{k-1}; \Delta z_i^{k-1}], \\ \mathbf{h}_i^k = \mathbf{h}_i^{k-1}, \mathbf{U}_i^k = \frac{1}{\lambda} \mathbf{U}_i^{k-1}, \mathbf{V}_i^k = \mathbf{V}_i^{k-1}. \end{cases}$$

where \mathbf{h}, \mathbf{U} , and \mathbf{V} are defined in (16).

For an arbitrary single time step, we have $rank(\mathbf{U}_i^k) = rank(\mathbf{R}_i^T \mathbf{A})$ as shown in (17). It can also be seen that $det(\mathbf{A}) = 0$ and the second-order sub-determinant of \mathbf{A} is not equal to 0, we know that $rank(\mathbf{A}) = 2$. \mathbf{R}_i^T is a rotation matrix, $rank(\mathbf{R}_i^T) = 3$, thus $rank(\mathbf{U}_i^k) = 2$. Therefore, $\bar{\mathbf{L}}_i$ will not be of full column rank.

(ii) When $\theta_{arr,j}^y = \frac{\pi}{2}$, for the corresponding microphone array at any different time steps, \mathbf{V}_i^k defined in (18) has the same structure, i.e.,

$$\mathbf{V}_i^k = \begin{bmatrix} 0 & \Delta x_i^k c_z + \Delta y_i^k s_z & 0 \\ \Delta y_i^k s_{x-z} - \Delta x_i^k c_{x-z} & \Delta z_i^k s_x & -\Delta y_i^k s_{x-z} + \Delta x_i^k c_{x-z} \\ \Delta y_i^k c_{x-z} + \Delta x_i^k s_{x-z} & \Delta z_i^k c_x & -\Delta y_i^k c_{x-z} - \Delta x_i^k s_{x-z} \end{bmatrix},$$

where s, c represent sin, cos , respectively and $rank(\mathbf{V}_i^k) \equiv 2$. Therefore, the matrix of $\bar{\mathbf{L}}_i$ in (20) will not be of full column rank. This completes the proof. ■